Mineralogical Magazine, October 2003, Vol. 67(5), pp. 1109–1120

The structure of hügelite, an arsenate of the phosphuranylite group, and its relationship to dumontite

A. J. Locock* and P. C. Burns

Department of Civil Engineering and Geological Sciences, University of Notre Dame, 156 Fitzpatrick Hall, Notre Dame, Indiana, 46556, USA

ABSTRACT

The crystal structure of hügelite, $Pb_2[(UO_2)_3O_2(AsO_4)_2](H_2O)_5$, monoclinic, space group $P2_1/m$, a = 31.066(3) Å, b = 17.303(2) Å, c = 7.043(1) Å, β = 96.492(2)°, V = 3761.6(1) Å^3, Z = 8, D_{calc} = 5.74 g/cm^3, was solved by direct methods using data from a crystal twinned by pseudo-merohedry, and was refined by full-matrix least-squares techniques on the basis of F^2 to agreement indices $R1$ of 3.3% calculated for 5519 unique observed reflections ($|F_o| \geqslant 4\sigma_F$), and wR_2 of 6.7% for all data. Intensity data were collected at room temperature using Mo-$K\alpha$ radiation and a CCD-based area detector. Hügelite is a member of the phosphuranylite group and is the arsenate counterpart of dumontite. The sheets of uranyl pentagonal and hexagonal bipyramids and arsenate tetrahedra in hügelite are oriented parallel to (100), and the interlayer contains four symmetrically independent Pb atoms, each of which is coordinated by two oxygen atoms from uranyl ions, two oxygen atoms from arsenate tetrahedra, and three symmetrically distinct H_2O groups. The unit-cell volume is four times larger than that previously reported for hügelite, or expected by comparison to dumontite, $Pb_2[(UO_2)_3O_2(PO_4)_2](H_2O)_5$; the larger cell probably results from the accommodation of the larger As atoms (relative to P) in the structure, and consequent subtle variations in the coordination geometries of the U and Pb positions.

Keywords: hügelite, phosphuranylite, uranyl arsenate, twin, crystal structure.

Introduction

Uranyl phosphates are amongst the most abundant and widespread of uranium mineral species, and together with the structurally corresponding uranyl arsenates, constitute about a third of the ~200 described uranium minerals (Finch and Murakami, 1999). Because of their low solubilities, these minerals are of considerable environmental importance for understanding the mobility of U in natural systems (Sowder *et al.*, 1996; Murakami *et al.*, 1997), and may control the concentration of U in groundwaters (Finch and Murakami, 1999). Uranyl arsenates are often structurally similar to their chemically corresponding uranyl phospates; cf. the isostructural species abernathyite, $K[(UO_2)(AsO_4)](H_2O)_3$, and meta-ankoleite, $K[(UO_2)(PO_4)](H_2O)_3$, (Ross and Evans, 1964; Fitch and Cole, 1991).

The phosphuranylite group is one of the two major groups of uranyl phosphate and uranyl arsenate minerals (autunite/meta-autunite being the other), and consists of at least sixteen minerals (Finch and Murakami, 1999; Burns, 1999). Hügelite and arsenuranylite are the only known arsenates of this group, and as part of our ongoing research into the structures of uranyl phosphates and uranyl arsenates (Locock and Burns, 2002*a,b*, 2003), we have determined the crystal structure of hügelite.

Previous studies

Hügelite was originally described by Dürrfeld (1913, 1914) as a lead zinc vanadate hydrate, but Walenta and Wimmenauer (1961) determined it to be a lead uranyl arsenate hydrate that is structurally related to dumontite, itself a lead

* E-mail: alocock@nd.edu
DOI: 10.1180/0026461036750146

uranyl phosphate hydrate of the phosphuranylite group (Piret and Piret-Meunier, 1988). Walenta (1979) re-investigated hügelite using material from the type locality of the Michael Mine at Weiler, near Lahr in the Black Forest, Baden-Württemberg, Federal Republic of Germany. He reported new morphologic data, physical and optical properties, the formula $Pb_2(UO_2)_3(AsO_4)_2(OH)_4{\cdot}3H_2O$, and the following crystallographic data: monoclinic, space group $P2_1/m$ or $P2_1$, a = 8.13 Å, b = 17.27 Å, c = 7.01 Å, β = 109º, Z = 2, D_{calc} = 5.80 g/cm^3.

Experimental

The hügelite sample studied is from the collection of the Mineralogical and Geological Museum of Harvard University, sample 98965. The sample is labelled as coming from 'Geroldseck, Baden' and is from the vicinity of the type locality.

Electron microprobe examination

The chemical composition of hügelite was confirmed by qualitative electron microprobe examination. Crystals of hügelite were mounted on an adhesive carbon tab and carbon coated. An energy-dispersive X-ray emission spectrum was acquired for 140 s with an ultrathin-window Si(Li) detector on a JEOL JXA-8600 Superprobe at an excitation voltage of 15 keV and a probe current of 1.3 nA. Following EDS examination, a wavelength-dispersive X-ray emission spectrum (Fig. 1) was acquired in the energy range 3.05–3.45 keV (PET crystal, excitation voltage 15 keV, probe current 28 nA, beam diameter 10 μm, step size 1.3 eV, count time 0.3 s per step) to check for the presence of K and resolve the potential overlap of the K-$K\alpha$ peak with that of U-$M\beta$. The only elements present were U, Pb, As, O and C; K was not detected.

Single-crystal X-ray diffraction

An optically homogeneous fragment of hügelite was mounted on a Bruker PLATFORM three-circle X-ray diffractometer operated at 50 keV and 40 mA and equipped with a 4K APEX CCD detector with a crystal to detector distance of 4.7 cm. A sphere of three-dimensional data was collected using graphite-monochromatized Mo-$K\alpha$ X-radiation and frame widths of 0.3º in ω, with count-times per frame of 120 s. Data were collected in 86 h for 4º ⩽ 2θ ⩽ 69º; comparison of the intensities of equivalent reflections measured at different times during data acquisition showed no significant decay. The unit cell (Table 1) was refined with 9590 reflections using least-squares techniques; its volume is four times larger than that reported by Walenta (1979) and is required by 8801 observed (mean I = 11.1 σ) reflections in the sphere of data. The intensity data were reduced and corrected for Lorentz, polarization, and background effects using the Bruker program SAINT. An empirical correction for

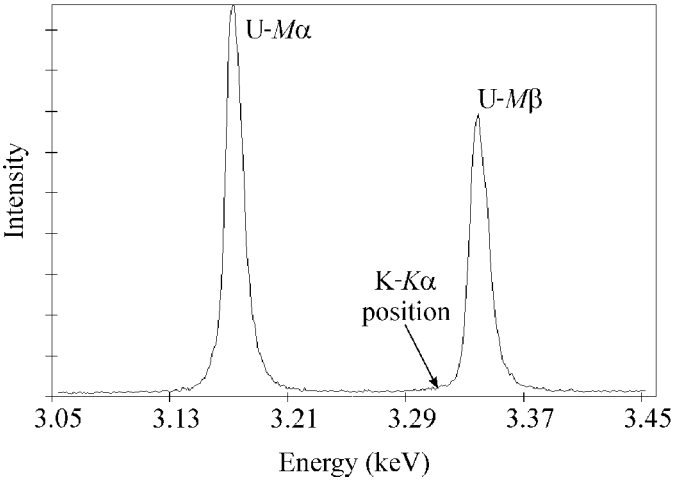

FIG. 1. Wavelength-dispersive X-ray emission spectrum of hügelite; the U-$M\alpha$ and U-$M\beta$ lines are well resolved and K-$K\alpha$ is not detected.

TABLE 1. Crystallographic data and details of the refinement foir hügelite.

a (Å)	31.066(3)
b (Å)	17.303(2)
c (Å)	7.043(1)
β (°)	96.492(2)
V (Å^3)	3761.6(1)
Space group	$P2_1/m$
Temperature (K)	293(2)
Formula (Z = 8)	$Pb_2[(UO_2)_3O_2(AsO_4)_2](H_2O)_5$
Formula weight (g/mol)	1624.4
Wavelength (Å)	0.71073
F(000)	5472
μ (mm^{-1})	47.18
D_{calc} (g/cm^3)	5.74
Crystal size (mm)	0.08 × 0.05 × 0.03
θ range of data collection	1.77 to 34.52°
Data collected	$-48 \leqslant h \leqslant 48$, $-26 \leqslant k \leqslant 27$, $-11 \leqslant l \leqslant 11$
Total reflections	77511
Unique reflections	16005
R_{int} (%)	11.3
Unique $\|F_o\| \geqslant 4\sigma_F$	5519
Completeness to θ = 34.52°	97.6%
Refinement method	Full-matrix least-squares on F^2
Parameters varied	322
$R1$ (%) for $\|F_o\| \geqslant 4\sigma_F$	3.3
$wR2$ (%) all data	6.7
Goodness of fit all data	0.68
Max. min. peaks (e/Å^3)	4.1, −2.9

$R1 = [\Sigma||F_o| - |F_c||]/\Sigma|F_o| \times 100$
$wR_2 = [\Sigma[w(F_o^2 - F_c^2)^2]/\Sigma[w(F_o^2)^2]]^{0.5} \times 100$
$w = 1/(\sigma^2(F_o^2) + (a \cdot P)^2$, $P = \frac{1}{3}\max(0,F_o^2) + \frac{2}{3}F_c^2$, $a = 0.0147$

absorption was applied using the program SADABS (G. Sheldrick, unpublished) on the basis of the intensities of equivalent reflections; this lowered R_{INT} of 15916 intense reflections from 17.4 to 9.6%. Systematic absences of reflections for hügelite were found to be consistent with space groups $P2_1/m$ or $P2_1$. A total of 77511 intensities was collected, of which 16005 are unique (R_{INT} = 11.3%), and 5519 are classified as observed reflections ($|F_o| \geqslant 4\sigma_F$). Scattering curves for neutral atoms, together with anomalous dispersion corrections, were taken from Ibers and Hamilton, 1974. The Bruker SHELXTL Version 5 series of programs was used for the solution and refinement of the crystal structure.

Structure solution and refinement

Direct methods were used to solve the structure of hügelite; the application of the twin law [$\bar{1}0\bar{1}$/010/001] was required to resolve the heavy atom (U, Pb, As) positions as the initial model gave unusually large uncertainties for interatomic distances and many significant electron-density peaks were present in the difference-Fourier map at locations incompatible with additional atomic sites. Refinement of the structure model showed that the crystal was twinned by pseudo-merohedry, which involved essentially complete overlap of the diffraction patterns that corresponded to each twin component. The monoclinic cell can be transformed to a C-centred pseudo-orthorhombic cell with dimensions a = 7.043 Å, b = 61.733 Å, c = 17.303 Å, γ = 90.02° using the matrix [00$\bar{1}$/201/0$\bar{1}$0]. The structure was refined according to published methods (Jameson, 1982; Herbst-Irmer and Sheldrick, 1998), on the basis of F^2 for all unique data in space group $P2_1/m$.

The structure model was slow to converge because of the large cell and pseudosymmetry present; in the final cycle of refinement, the mean shift/esd was 0.140, and the maximum peaks in the final difference-Fourier maps were 4.1 and

-2.9 e/Å^3. A structure model including the twin law and anisotropic displacement parameters for all non-O atoms gave an agreement index ($R1$) of 3.3%, calculated for the 5519 observed unique reflections ($|F_o| \geqslant 4\sigma_F$), whereas removal of the twin law from the otherwise identical model yielded an agreement index ($R1$) of 47%. The twin-component scale factor refined to 0.4545(3). The final value of wR_2 was 6.7% for all data using the structure-factor weights assigned during least-squares refinement. The locations of the H atoms in the unit cell were not determined.

The larger cell found in this work can be transformed to the smaller cell of Walenta (1979) using the matrix [¼0½/0$\bar{1}$0/00$\bar{1}$]. The relationship between the two unit cells is shown in Fig. 2. For comparative purposes, a solution was undertaken in space group $P2_1/m$ in the smaller cell: a = 8.157 Å, b = 17.303 Å, c = 7.043 Å, β = 108.91º. This model yielded an agreement index ($R1$) of 16.9%, but gave unreasonable displacement parameters for some of the O atoms, and generated significant electron-density peaks in the difference-Fourier maps at locations incompatible with additional atomic sites. Moreover, the larger 31.066 Å unit cell is required by 8801 observed ($I > 3\sigma$) reflections in the sphere of data, and therefore the smaller 8.157 Å cell cannot be warranted.

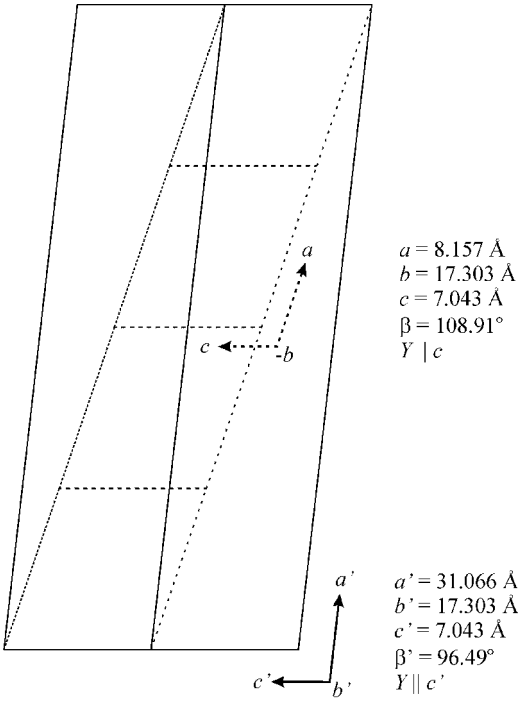

FIG. 2. Projection along [010] of the relationship between the unit-cell equivalent to that of Walenta (1979), a b c β (shown in black stipple), and the larger unit cell, a' b' c' β' (denoted by ') presented in this work.

The positional parameters and anisotropic displacement parameters of atoms in hügelite are given in Tables 2 and 3 respectively, and selected interatomic distances and angles are given in Table 4. Observed and calculated structure factors have been deposited with the editorial office of *Mineralogical Magazine*, and are available from the Mineralogical Society website www.minersoc.org/pages/e_journals/dep_mat.htm

Bond-valence sums were calculated using the parameters of Burns *et al.* (1997) for U, Krivovichev and Filatov (2001) for Pb, and Brown and Altermatt (1985) for As. At the U sites, the bond valence sums range from 5.8 to 6.4 valence units, whereas the sums at the Pb and As sites range from 1.7 to 1.9, and 4.7 to 5.4 valence units, respectively. These results are consistent with formal valences of U^{6+}, Pb^{2+} and As^{5+}. The bond valence sums for sites OW41 to OW52 range from 0.2 to 0.3 valence units, consistent with their assignment as H_2O groups. The bond valence sums for the forty remaining O atoms range from 1.5 to 2.2 valence units. The bond valence analysis of hügelite yields the formula $Pb_2[(UO_2)_3O_2(AsO_4)_2](H_2O)_5$, at variance with that of Walenta (1979), but similar to that reported for dumontite, $Pb_2[(UO_2)_3O_2(PO_4)_2](H_2O)_5$ (Piret and Piret-Meunier, 1988).

Description of the structure

The structure of hügelite is shown projected along [100] in Fig. 3. As with other structures of the phosphuranylite group (see Burns, 1999), hügelite contains sheets based upon the phosphuranylite sheet-anion topology (Fig. 4), in this case consisting of uranyl polyhedra and arsenate tetrahedra; Pb and H_2O groups occur in the interlayer. There are eight symmetrically independent U atoms in hügelite, each of which is part of an approximately linear $(UO_2)^{2+}$ cation. The uranyl ions of U1, U2, U3 and U4 are coordinated by six additional O atoms arranged at the equatorial positions of hexagonal bipyramids, with the uranyl ion O atoms at the apices of the bipyramids, whereas the uranyl ions of U5, U6, U7 and U8 are coordinated in a similar fashion by

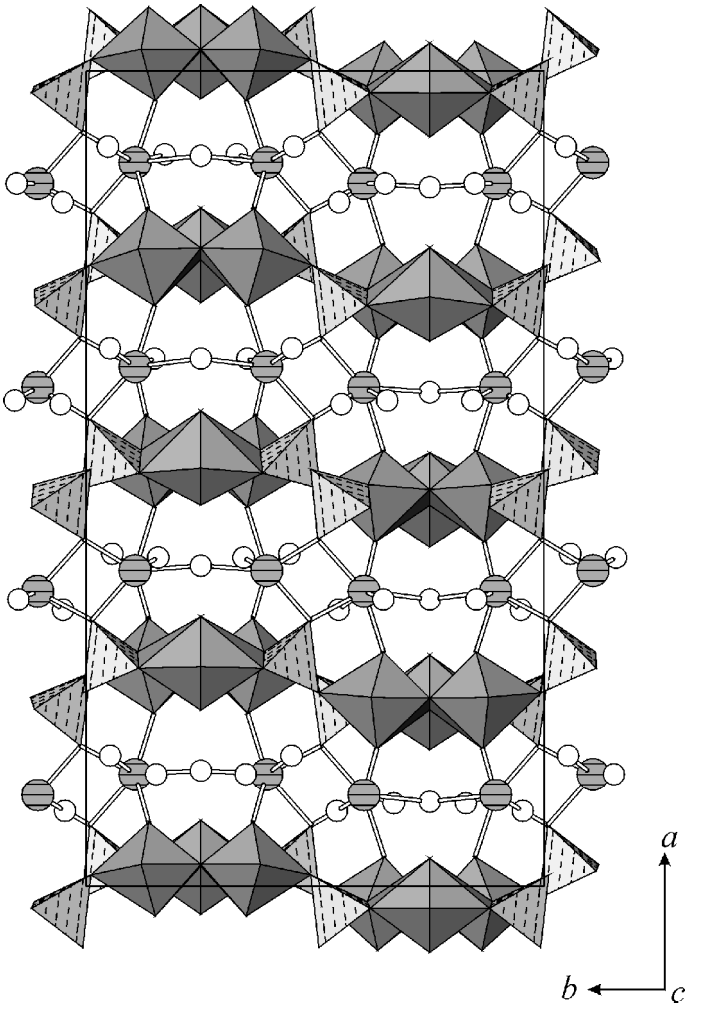

FIG. 3. Polyhedral representation of the crystal structure of hügelite projected along [001]. The uranyl polyhedra are shaded and the arsenate tetrahedra are stippled. The Pb atoms are shown as striped spheres, and the H_2O groups as unfilled spheres.

five additional O atoms arranged at the equatorial positions of pentagonal bipyramids (Table 4). The uranyl pentagonal bipyramids share equatorial edges with each other and with the hexagonal bipyramids to form chains that have a ratio of pentagonal bipyramids to hexagonal bipyramids of 2:1. Each of the four symmetrically distinct arsenate tetrahedra shares an edge with a hexagonal bipyramid, and its opposite corner with a pentagonal bipyramid, thus serving to link the offset chains of uranyl polyhedra into sheets (Fig. 4). The interlayer of hügelite contains four symmetrically independent Pb positions and twelve distinct H_2O groups. As in dumontite (Piret and Piret-Meunier, 1988), all of the Pb positions are in 7-fold coordination (Table 4); each is coordinated by two oxygen atoms from uranyl ions, two oxygen atoms from arsenate tetrahedra, and three H_2O groups (Fig. 5).

Discussion

The relationship of hügelite to dumontite

Chemically, hügelite is the As analogue of dumontite, but these species are not isostructural, although various uranyl arsenates of the meta-

TABLE 2. Atomic coordinates and isotropic displacement parameters ($Å^2 \times 10^3$) for hügelite.

	x	*y*	*z*	U_{eq}*
U1	0.0240(1)	¾	0.2750(3)	13(1)
U2	−0.2261(1)	¾	0.5247(3)	14(1)
U3	−0.2741(1)	¼	−0.0251(3)	14(1)
U4	−0.4761(1)	¾	−0.2247(3)	14(1)
U5	0.0216(1)	0.6446(1)	0.7748(2)	11(1)
U6	−0.2285(1)	0.6446(1)	0.0249(2)	11(1)
U7	−0.2715(1)	0.3553(1)	0.4748(2)	11(1)
U8	−0.4785(1)	0.6445(1)	−0.7257(2)	11(1)
Pb1	−0.3624(1)	0.6065(1)	−0.0037(3)	23(1)
Pb2	−0.1377(1)	0.3938(1)	0.5037(3)	23(1)
Pb3	−0.3877(1)	0.3938(1)	0.7541(3)	23(1)
Pb4	−0.1122(1)	0.6062(1)	0.7465(3)	22(1)
As1	0.0281(1)	0.5524(2)	0.2816(6)	12(1)
As2	−0.2217(1)	0.5515(2)	0.5298(6)	15(1)
As3	−0.2782(1)	0.4478(2)	−0.0299(5)	12(1)
As4	−0.4719(1)	0.5515(2)	−0.2202(6)	16(1)
O1	0.0807(11)	¾	0.3320(50)	22(8)
O2	−0.0344(10)	¾	0.2170(40)	16(7)
O3	−0.2849(12)	¾	0.4740(50)	28(8)
O4	−0.1678(13)	¾	0.5790(60)	39(11)
O5	−0.3312(13)	¼	−0.0760(60)	20(10)
O6	−0.2171(14)	¼	0.0260(60)	19(11)
O7	−0.5320(11)	¾	−0.2650(50)	31(9)
O8	−0.4161(12)	¾	−0.1720(50)	25(9)
O9	0.0782(8)	0.6364(15)	0.7660(40)	30(7)
O10	−0.0362(6)	0.6509(10)	0.7570(30)	18(4)
O11	−0.02877(8)	0.6488(14)	0.0270(40)	16(6)
O12	−0.1688(5)	0.6342(10)	0.0210(30)	6(3)
O13	−0.3295(7)	0.3645(12)	0.4560(30)	33(6)
O14	−0.2124(6)	0.3526(10)	0.4550(30)	12(4)
O15	−0.5349(8)	0.6489(14)	−0.7150(40)	33(7)
O16	−0.4220(7)	0.6304(12)	−0.7430(30)	20(5)
O17	0.0245(7)	¾	0.5930(30)	2(4)
O18	0.0270(10)	¾	−0.0450(50)	16(7)
O19	0.0267(4)	0.6196(8)	0.1080(19)	6(3)
O20	0.0184(8)	0.6144(14)	0.4520(40)	26(6)
O21	−0.2312(12)	¾	−0.1650(50)	23(9)
O22	−0.2171(9)	¾	0.2120(40)	10(6)
O23	−0.2325(5)	0.6216(8)	0.6870(20)	5(3)
O24	−0.2175(8)	0.6131(13)	0.3480(30)	24(6)
O25	−0.2768(9)	¼	0.2880(40)	9(6)
O26	−0.2703(10)	¼	0.6520(40)	8(6)
O27	−0.2681(8)	0.3869(13)	−0.1990(30)	26(6)
O28	−0.2878(6)	0.3879(11)	0.1450(30)	15(4)
O29	−0.4674(11)	¾	−0.5400(50)	21(8)
O30	−0.4871(8)	¾	0.0830(30)	15(5)
O31	−0.4929(4)	0.6152(7)	−0.0551(18)	14(3)
O32	−0.4650(8)	0.6204(13)	−0.3870(30)	27(6)
O33	0.0752(7)	0.5079(13)	0.3580(30)	17(5)
O34	−0.0141(5)	0.4902(9)	0.2460(20)	14(3)
O35	−0.1727(5)	0.5123(8)	0.5667(19)	14(3)
O36	−0.2625(7)	0.4909(13)	0.4610(30)	14(5)
O37	−0.2381(8)	0.5072(15)	0.0250(30)	20(6)
O38	−0.3268(7)	0.4881(12)	−0.0980(30)	17(5)
O39	−0.5119(7)	0.4903(13)	−0.2830(30)	14(5)
O40	−0.4260(8)	0.5052(13)	−0.1340(40)	32(6)

TABLE 2. (*contd.*)

	x	*y*	*z*	U_{eq}*
OW41	−0.3523(9)	¾	0.1820(40)	13(6)
OW42	−0.1423(12)	¼	0.2920(50)	53(10)
OW43	−0.3940(13)	¼	0.5710(60)	39(10)
OW44	−0.1044(12)	¾	0.9330(50)	17(9)
OW45	−0.1603(9)	0.4479(16)	0.1730(40)	36(7)
OW46	−0.3396(9)	0.5492(16)	0.3270(40)	31(8)
OW47	−0.0925(9)	0.5486(15)	0.0830(40)	32(7)
OW48	−0.4086(7)	0.4434(10)	0.3860(30)	35(5)
OW49	−0.4038(8)	0.3431(14)	0.1000(40)	43(6)
OW50	−0.1020(7)	0.6713(9)	0.4030(30)	35(4)
OW51	−0.3524(10)	0.6482(17)	−0.3600(50)	64(10)
OW52	−0.1378(6)	0.3477(11)	0.8650(30)	34(4)

*U_{eq} is defined as one third of the trace of the orthogonalized U_{ij} tensor.

autunite group are isostructural with their phosphate analogues, including the K, NH_4 and H_3O members (Ross and Evans, 1964; Fitch and Cole, 1991; Fitch and Fender, 1983; Fitch *et al.*, 1983; Morosin, 1978). The unit-cell volume of hügelite is four times larger than that previously reported (Walenta, 1979), or expected by comparison with dumontite (Piret and Piret-Meunier, 1988). The structure of hügelite is closely related to that of dumontite, and the subcell of hügelite (Fig. 2) corresponds to the cell of dumontite (Piret and Piret-Meunier, 1988). The uranyl arsenate sheet in hügelite (Fig. 4) is the same geometrical isomer as the uranyl phosphate sheet in dumontite and vanmeersscheite (Piret and Deliens, 1982; Piret and Piret-Meunier, 1988): tetrahedra between the chains of uranyl polyhedra alternate orientations in an up-down up-down pattern, and each pair of tetrahedra attached to a given uranyl hexagonal bipyramid has the same orientation (Burns, 1999).

TABLE 3. Anisotropic displacement parameters ($Å^2 \times 10^3$) for hügelite.

	U_{11}	U_{22}	U_{33}	U_{23}	U_{13}	U_{12}
U1	11(1)	18(1)	11(1)	0	0(1)	0
U2	14(1)	16(1)	10(1)	0	0(1)	0
U3	17(1)	13(1)	11(1)	0	2(1)	0
U4	19(1)	11(1)	10(1)	0	−1(1)	0
U5	8(1)	12(1)	11(1)	0(1)	0(1)	0(1)
U6	14(1)	9(1)	11(1)	0(1)	2(1)	−1(1)
U7	14(1)	7(1)	12(1)	−1(1)	2(1)	1(1)
U8	15(1)	8(1)	11(1)	0(1)	2(1)	−1(1)
Pb1	20(1)	21(1)	27(1)	1(1)	2(1)	−1(1)
Pb2	17(1)	22(1)	29(1)	0(1)	2(1)	−1(1)
Pb3	19(1)	22(1)	27(1)	0(1)	2(1)	−2(1)
Pb4	14(1)	24(1)	29(1)	−1(1)	1(1)	−1(1)
As1	16(2)	4(2)	15(2)	−2(2)	0(2)	−6(1)
As2	17(2)	9(2)	17(2)	−1(2)	1(2)	1(2)
As3	19(2)	7(2)	9(2)	−1(2)	−3(2)	−2(2)
As4	(22(2)	18(2)	10(2)	2(2)	5(2)	2(2)

The anisotropic displacement parameter exponent takes the form: $-2\pi^2 [h^2\mathbf{a}^{*2}U_{11} + ... + 2\ hk\mathbf{a}^*\ \mathbf{b}^*\ U_{12}]$.

The effective ionic radius of $^{[4]}As^{5+}$ is essentially double that of $^{[4]}P^{5+}$ (Shannon, 1976). Accommodation of the larger As atoms in hügelite presumably results in the larger unit cell, and consequent variations in the coordination geometries of the U and Pb positions. Such an accommodation is probably less easily made in the phosphuranylite-type sheet, which involves extensive sharing of polyhedral edges, (Fig. 4), than in the autunite sheet, which involves only the sharing of vertices between polyhedra (Burns, 1999). Vertex-sharing of polyhedra of higher bond-valence permits a greater degree of structural flexibility than does edge-sharing.

In hügelite, the average As–O bond distances per tetrahedron range from 1.65 to 1.71 Å (Table 4), whereas the mean P–O distance in dumontite is ~10% smaller at 1.52 Å (Piret and Piret-Meunier, 1988). The arsenate tetrahedra in hügelite are more distorted than the phosphate tetrahedron in dumontite. Amongst the four symmetrically independent arsenate tetrahedra, the ranges of interatomic distances and angles vary from 0.03 to 0.12 Å, and 14 to 25°,

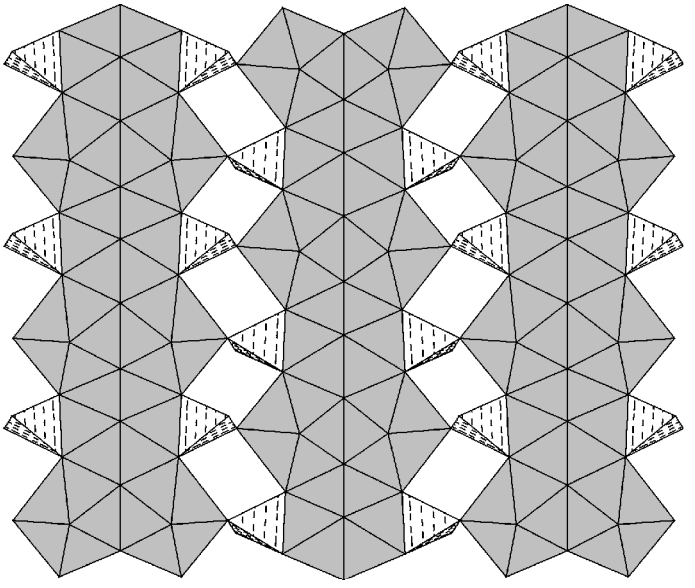

FIG. 4. The uranyl arsenate sheet of hügelite, projected parallel to [100]. The uranyl polyhedra are shaded and the arsenate tetrahedra are stippled.

respectively (Table 4), whereas the phosphate tetrahedron in dumontite shows a range in bond lengths of 0.06 Å, and a range in angles of 15º (Piret and Piret-Meunier, 1988).

The large unit cell of hügelite is associated with subtle variations in the coordination environments of the symmetrically independent U and Pb positions (Table 4). It is instructive to examine the variation in interatomic distances and angles between the Pb positions and oxygen atoms from uranyl ions (O_{ap}) shown in Fig. 5. The Pb1 position is bonded to two O_{ap}: O11 –2.42 Å,

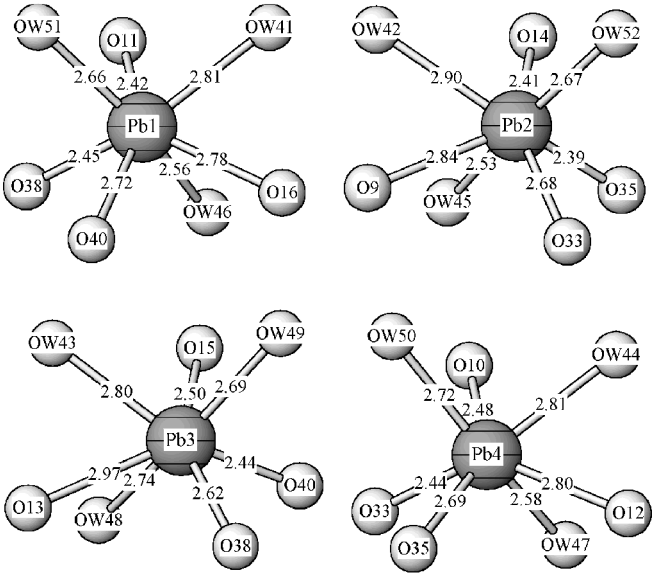

FIG. 5. The four Pb positions in hügelite, showing the variation in interatomic distances of their coordination environments.

TABLE 4. Selected interatomic distances (Å) and angles (º) for hügelite.

U1–O1	1.76(3)			U4–O7	1.73(4)		
U1–O2	1.81(3)	O1–U1–O2	179.7(15)	U4–O8	1.86(4)	O7–U4–O8	178.1(15)
U1–O17	2.24(2)	O1–U1–O17	82.9(12)	U4–O30	2.23(2)	O7–U4–O30	84.2(13)
U1–O18	2.27(3)	O1–U1–O18	94.3(14)	U4–O29	2.27(3)	O7–U4–O29	93.8(14)
U1–O19	2.55(1) × 2	O1–U1–O19	91.2(6) × 2	U4–O32	2.56(2) × 2	O7–U4–O32	96.3(8) × 2
U1–O20	2.67(2) × 2	O1–U1–O20	90.5(8) × 2	U4–O31	2.70(1) × 2	O7–U4–O31	80.3(6) × 2
<U1–O_{ap}>	1.79			<U4–O_{ap}>	1.80		
<U1–O_{eq}>	2.49			<U4–O_{eq}>	2.50		
U2–O3	1.82(4)			U5–O9	1.77(3)		
U2–O4	1.81(4)	O3–U2–O4	179.1(17)	U5–O10	1.79(2)	O9–U5–O10	173.8(10)
U2–O21	2.21(4)	O3–U2–O21	90.6(15)	U5–O18	2.22(2)	O9–U5–O18	94.3(12)
U2–O22	2.25(3)	O3–U2–O22	92.4(13)	U5–O17	2.24(1)	O9–U5–O17	86.5(10)
U2–O23	2.52(2) × 2	O3–U2–O23	87.7(6) × 2	U5–O34	2.35(2)	O9–U5–O34	90.6(9)
U2–O24	2.70(2) × 2	O3–U2–O24	93.4(7) × 2	U5–O20	2.32(3)	O9–U5–O20	83.0(11)
<U2–O_{ap}>	1.82			U5–O19	2.37(1)	O9–U5–O19	93.8(9)
<U2–O_{eq}>	2.48			<U5–O_{ap}>	1.78		
				<U5–O_{eq}>	2.23		
U3–O5	1.77(4)			U6–O11	1.84(2)		
U3–O6	1.77(4)	O5–U3–O6	180.0(18)	U6–O12	1.86(2)	O11–U6–O12	176.7(9)
U3–O25	2.22(3)	O5–U3–O25	93.0(15)	U6–O21	2.26(2)	O11–U6–O21	90.1(12)
U3–O26	2.29(3)	O5–U3–O26	87.9(15)	U6–O22	2.25(2)	O11–U6–O22	93.1(10)
U3–O27	2.68(2) × 2	O5–U3–O27	91.6(8) × 2	U6–O24	2.33(2)	O11–U6–O24	92.2(10)
U3–O28	2.73(2) × 2	O5–U3–O28	83.4(7) × 2	U6–O37	2.40(3)	O11–U6–O37	85.1(10)
<U3–O_{ap}>	1.77			U6–O23	2.40(1)	O11–U6–O23	94.2(9)
<U3–O_{eq}>	2.56			<U6–O_{ap}>	1.85		
				<U6–O_{eq}>	2.33		
U7–O13	1.80(2)			Pb2–O14	2.41(2)		
U7–O14	1.86(2)	O13–U7–O14	170.8(9)	Pb2–O35	2.39(1)	O14–Pb2–O35	80.2(6)
U7–O26	2.20(2)	O13–U7–O26	93.9(10)	Pb2–OW45	2.53(3)	O14–Pb2–OW45	79.5(8)
U7–O25	2.24(2)	O13–U7–O25	91.3(10)	Pb2–OW52	2.67(2)	O14–Pb2–OW52	86.7(6)
U7–O27	2.35(2)	O13–U7–O27	89.2(9)	Pb2–O33	2.68(2)	O14–Pb2–O33	152.1(6)
U7–O36	2.37(2)	O13–U7–O36	91.8(9)	Pb2–O9	2.84(3)	O14–Pb2–O9	122.6(7)
U7–O28	2.39(2)	O13–U7–O28	78.8(8)	Pb2–OW42	2.90(2)	O14–Pb2–OW42	71.5(8)
<U7–O_{ap}>	1.83			<Pb2–O>	2.63		
<U7–O_{eq}>	2.31						
U8–O15	1.76(2)			Pb3–O15	2.50(2)		
U8–O16	1.79(2)	O15–U8–O16	174.4(10)	Pb3–O40	2.44(2)	O15–Pb3–O40	76.8(8)
U8–O29	2.25(2)	O15–U8–O29	91.6(12)	Pb3–O38	2.62(2)	O15–Pb3–O38	150.3(8)
U8–O30	2.27(2)	O15–U8–O30	86.5(10)	Pb3–OW49	2.69(2)	O15–Pb3–OW49	74.3(8)
U8–O39	2.35(2)	O15–U8–O39	85.0(10)	Pb3–OW48	2.74(2)	O15–Pb3–OW48	82.3(8)
U8–O31	2.37(1)	O15–U8–O31	88.4(10)	Pb3–OW43	2.80(2)	O15–Pb3–OW43	70.8(10)
U8–O32	2.41(2)	O15–U8–O32	91.6(11)	Pb3–O13	2.97(2)	O15–Pb3–O13	121.8(7)
<U8–O_{ap}>	1.78			<Pb3–O>	2.68		
<U8–O_{eq}>	2.33						
Pb1–O11	2.42(2)			Pb4–O10	2.48(2)		
Pb1–O38	2.45(2)	O11–Pb1–O38	79.7(8)	Pb4–O33	2.44(2)	O10–Pb4–O33	77.3(7)
Pb1–OW46	2.56(3)	O11–Pb1–OW46	82.7(9)	Pb4–OW47	2.58(3)	O10–Pb4–OW47	88.0(7)
Pb1–OW51	2.66(3)	O11–Pb1–OW51	77.8(9)	Pb4–O35	2.69(1)	O10–Pb4–O35	144.6(5)
Pb1–O40	2.72(2)	O11–Pb1–O40	151.4(8)	Pb4–OW50	2.72(2)	O10–Pb4–OW50	72.0(6)
Pb1–O16	2.78(2)	O11–Pb1–O16	126.8(8)	Pb4–O12	2.80(2)	O10–Pb4–O12	126.6(6)
Pb1–OW41	2.81(1)	O11–Pb1–OW41	68.6(8)	Pb4–OW44	2.81(2)	O10–Pb4–OW44	71.2(9)
<Pb1–O>	2.63			<Pb3–O>	2.64		
As1–O20	1.66(2)	O19–As1–O34	112.1(7)	As3–O37	1.63(3)	O27–As3–O38	107.3(11)
As1–O33	1.68(2)	O20–As1–O19	94.9(10)	As3–O28	1.66(2)	O28–As3–O27	101.6(11)
As1–O19	1.69(1)	O20–As1–O33	106.6(12)	As3–O27	1.65(2)	O28–As3–O38	103.9(10)
As1–O34	1.69(2)	O20–As1–O34	108.3(10)	As3–O38	1.68(2)	O37–As3–O27	111.9(12)
<As1–O>	1.68	O33–As1–O19	119.9(10)	<As3–O>	1.65	O37–As3–O28	114.4(11)
		O33–As1–O34	112.7(10)			O37–As3–O38	116.4(12)
As2–O35	1.66(2)	O24–As2–O23	94.7(10)	As4–O39	1.66(2)	O32–As4–O31	95.8(9)
As2–O36	1.67(2)	O35–As2–O23	115.7(7)	As4–O40	1.69(2)	O39–As4–O31	104.4(9)
As2–O24	1.68(2)	O35–As2–O24	103.2(10)	As4–O32	1.70(2)	O39–As4–O32	114.4(11)
As2–O23	1.70(1)	O35–As2–O36	116.1(9)	As4–O31	1.78(1)	O39–As4–O40	111.8(12)
<As2–O>	1.68	O36–As2–O23	115.9(9)	<As4–O>	1.71	O40–As4–O31	114.6(10)
		O36–As2–O24	107.4(11)			O40–As4–O32	114.5(12)

and O16 –2.78 Å, and the O11–Pb1–O16 angle is 127° (Table 4). Similarly, the Pb2 position is bonded to O14 –2.41 Å, and O9 –2.84 Å, with an O14–Pb2–O9 angle of 123°. The Pb3 position is bonded to O15 –2.50 Å, and O13 –2.97 Å, with an O15–Pb3–O13 angle of 122°, whereas the Pb4 position is bonded to O10 –2.48 Å, and O12 –2.80, with an O10–Pb4–O12 angle of 127°. The four shorter Pb–O_{ap} bonds show a range of 0.09 Å, the longer Pb–O_{ap} bonds have a range of 0.19 Å, and the O_{ap}–Pb–O_{ap} angles show a range of 5°. This variability is outside of experimental uncertainty.

Structural relations in other Pb uranyl phosphates and arsenates

The considerable change in cell volume observed in the transition from dumontite (P end-member) to hügelite (As end-member) does not appear to be a general feature of other lead uranyl phosphate and arsenate series, but the paucity of structure refinements in these chemical systems does not permit certainty in this regard.

In contrast to the dumontite–hügelite chemical series, the series parsonsite–hallimondite {$Pb_2(UO_2)(PO_4)_2$ and $Pb_2(UO_2)(AsO_4)_2$, respectively}, have similar cell dimensions and volumes, although the structure of hallimondite has not yet been determined. The structure of parsonsite, is based on chains that consist of dimers of uranyl pentagonal bipyramids that are cross-linked by edge- and vertex-sharing with phosphate tetrahedra. Six- and nine-coordinate Pb atoms link adjacent uranyl phosphate chains (Burns, 2000). Its arsenate counterpart hallimondite is expected to be isostructural; it is likely that the chain structure can more easily accommodate As than the phosphuranylite-type sheet found in dumontite and hügelite. Interestingly, hallimondite and hügelite are described from the same type locality (Walenta, 1965).

In the meta-autunite group, przhevalskite, $Pb[(UO_2)(PO_4)]_2(H_2O)_4$, (Pekov, 1998; Finch and Murakami, 1999), has a synthetic arsenate analogue (Powder Diffraction File 26-1161), but an equivalent arsenate mineral species has not yet been described. These compounds differ considerably in their reported cell dimensions and volumes, but given the pseudo-symmetry prevalent in the autunite and meta-autunite groups (e.g. Locock and Burns, 2003), and the absence of refined structures for these compounds, no conclusions can be reached on the role of As for P substitution in this series. Meta-autunite group structures contain the well-known autunite-type sheet that consists of $(UO_2)O_4$ square bipyramids sharing equatorial vertices with phosphate or arsenate tetrahedra, and their interlayers contain monovalent, divalent or trivalent cations along with differing numbers of H_2O groups (Burns, 1999).

No arsenate equivalent of dewindtite, $Pb_3[(UO_2)_3O(OH)(PO_4)_2]_2(H_2O)_{12}$, the only other lead uranyl phosphate hydrate of the phosphuranylite group, has yet been described or synthesized. Dewindtite differs from dumontite in composition, symmetry, cell dimensions, and uranyl phosphate sheet geometry (Piret *et al.*, 1990); in the phosphuranylite-type sheet found in dewindtite, the tetrahedra change orientation in an up-up down-down sequence, and the tetrahedra attached to the same uranyl hexagonal bipyramid have the same orientation. However, based on the presence of phosphuranylite-type sheets in both dumontite and dewindtite, one might expect similar behaviour with regard to As substitution; the As analogue of dewindtite can be predicted to have a considerably larger cell, in the same fashion as hügelite has a considerably larger cell than dumontite.

Acknowledgements

We are grateful to Carl A. Francis and the Mineralogical and Geological Museum of Harvard University for the loan of the specimen. We are indebted to Sergey Krivovichev for his assistance with the twinning. We thank Jinesh Jain for assistance with the electron-microprobe data acquisition. The authors thank an anonymous reviewer, Robert Shuvalov, and associate editor Mark D. Welch for their comments on the manuscript. AJL thanks the Mineralogical Association of Canada for the MAC Foundation 2001 Scholarship. This research was supported by the Environmental Management Science Program of the Office of Science, U.S. Department of Energy, grants DE-FGO7-97ER14820 and DE-FGO7-02ER63489.

References

Brown, I.D. and Altermatt, D. (1985) Bond-valence parameters obtained from a systematic analysis of the inorganic crystal structure database. *Acta Crystallographica*, **B41**, 244–247.

Burns, P.C. (1999) The crystal chemistry of uranium.

Pp. 23–90 in: *Uranium: Mineralogy, Geochemistry and the Environment* (P.C. Burns and R. Finch, editors). Reviews in Mineralogy, **38**. Mineralogical Society of America, Washington D.C.

Burns, P.C. (2000) A new uranyl phosphate chain in the structure of parsonsite. *American Mineralogist*, **85**, 801–805.

Burns, P.C., Ewing, R.C. and Hawthorne, F.C. (1997) The crystal chemistry of hexavalent uranium: polyhedron geometries, bond-valence parameters, and polymerization of polyhedra. *The Canadian Mineralogist*, **35**, 1551–1570.

Dürrfeld, V. (1913) Über Krystalle eines wasserhaltigen Blei-Zink-Vanadinits von Reichenbach bei Lahr (Schwarzwald). [Translation: On a crystal of water-bearing lead zinc vanadate from Reichenbach near Lahr (Black Forest)]. *Zeitschrift für Kristallographie*, **51**, 278–279.

Dürrfeld, V. (1914) Über einige bemerkenswerte Mineralvorkommen des Kinzigtales (Schwarzwald). 4. Hügelit, ein neues wasserhaltiges Blei-Zink-Vanadinit von Reichenbach bei Lahr. [Translation: On the remarkable mineral occurrences of Kinzigtales (Black Forest). 4. Hügelite, a new water-bearing lead zinc vanadate from Reichenbach near Lahr.] *Zeitschrift für Kristallographie*, **53**, 182–183.

Finch, R. and Murakami, T. (1999) Systematics and paragenesis of uranium minerals. Pp. 91–180 in: *Uranium: Mineralogy, Geochemistry and the Environment* (P.C. Burns and R. Finch, editors). Reviews in Mineralogy, **38**. Mineralogical Society of America, Washington D.C.

Fitch, A.N. and Cole, M. (1991) The structure of $KUO_2PO_4.3D_2O$ refined from neutron and synchrotron-radiation powder diffraction data. *Material Science Research Bulletin*, **26**, 407–414.

Fitch, A.N. and Fender, B.E.F. (1983) The structure of deuterated ammonium uranyl phosphate trihydrate, $ND_4UO_2PO_4{\cdot}3D_2O$ by powder neutron diffraction. *Acta Crystallographica*, **C39**, 162–166.

Fitch, A.N., Bernard, L., Howe, A.T., Wright, A.F. and Fender, B.E.F. (1983) The room-temperature structure of $DUO_2AsO_4{\cdot}4D_2O$ by powder neutron diffraction. *Acta Crystallographica*, **C39**, 159–162.

Herbst-Irmer, R. and Sheldrick, G.M. (1998) Refinement of twinned structures with *SHELXL97*. *Acta Crystallographica*, **B54**, 443–449.

Ibers, J.A. and Hamilton, W.C., editors (1974) *International Tables for X-ray Crystallography*, **IV.** The Kynoch Press, Birmingham, UK.

Jameson, G.B. (1982) On structure refinement using data from a twinned crystal. *Acta Crystallographica,* **A38**, 817–820.

Krivovichev, S.V. and Filatov, S.K. (2001) *Crystal Chemistry of Minerals and Inorganic Compounds with Complexes of Anion-Centered Tetrahedra.* Saint Petersburg State University, Saint Petersburg, Russia, 122 pp. (in Russian).

Locock, A.J. and Burns, P.C. (2002*a*) The crystal structure of triuranyl diphosphate tetrahydrate. *Journal of Solid State Chemistry*, **163**, 275–280.

Locock, A.J. and Burns, P.C. (2002*b*) Crystal structures of three framework alkali metal uranyl phosphate hydrates. *Journal of Solid State Chemistry*, **167**, 226–236.

Locock, A.J. and Burns, P.C. (2003) The crystal structure of synthetic autunite, $Ca[(UO_2)(PO_4)]_2(H_2O)_{11}$. *American Mineralogist*, **88**, 240–244.

Morosin, B. (1978) Hydrogen uranyl phosphate tetrahydrate, a hydrogen ion solid electrolyte. *Acta Crystallographica*, **B34**, 3732–3734.

Murakami, T., Ohnuki, T., Isobe, H. and Tsutomu, T. (1997) Mobility of uranium during weathering. *American Mineralogist*, **82**, 888–899.

Pekov, I. (1998) *Minerals First Discovered on the Territory of the former Soviet Union*. Ocean Pictures Ltd., Moscow, 369 pp.

Piret, P. and Deliens, M. (1982) La vanmeersscheite $U(UO_2)_3(PO_4)_2(OH)_6{\cdot}4H_2O$ et la méta-vanmeersscheite $U(UO_2)_3(PO_4)_2(OH)_6{\cdot}2H_2O$. [Translation: Vanmeersscheite $U(UO_2)_3(PO_4)_2(OH)_6{\cdot}4H_2O$ and metavanmeersscheite $U(UO_2)_3(PO_4)_2(OH)_6{\cdot}2H_2O$.] *Bulletin de Minéralogie*, **105**, 125–128.

Piret, P. and Piret-Meunier, J. (1988) Nouvelle détermination de la structure cristalline de la dumontite $Pb_2[(UO_2)_3O_2(PO_4)_2]{\cdot}5H_2O$. [Translation: A new determination of the crystal structure of dumontite $Pb_2[(UO_2)_3O_2(PO_4)_2]{\cdot}5H_2O$.] *Bulletin de Minéralogie*, **111**, 439–442.

Piret, P., Piret-Meunier, J. and Deliens, M. (1990) Composition chimique et structure cristalline de la dewindtite $Pb_3[H(UO_2)_3O_2(PO_4)_2]_2{\cdot}12H_2O$. [Translation: The chemical composition and crystal structure of dewindtite $Pb_3[H(UO_2)_3O_2(PO_4)_2]_2{\cdot}12H_2O$.] *European Journal of Mineralogy*, **2**, 399–405.

Ross, M. and Evans, H.T. (1964) Studies of the torbernite minerals (I): the crystal structure of abernathyite and the structurally related compounds $NH_4(UO_2AsO_4){\cdot}3H_2O$ and $K(H_3O)(UO_2AsO_4)_2{\cdot}6H_2O$. *American Mineralogist*, **49**, 1578–1602.

Shannon, R.D. (1976) Revised effective ionic radii and systematic studies of interatomic distances in halide and chalcogenides. *Acta Crystallographica*, **A32**, 751–767.

Sowder, A.G., Clark, S.B. and Fjeld, R.A. (1996) The impact of mineralogy in the U(VI)-Ca-PO_4 system on the environmental availability of uranium. *Journal of Radioanalytical and Nuclear Chemistry*,

248, 517–524.

Walenta, K. (1965) Hallimondite, a new uranium mineral from the Michael Mine near Reichenbach (Black Forest, Germany). *American Mineralogist*, **50**, 1143–1157.

Walenta, K. (1979) Über den Hügelit. [Translation: Hügelite.] *Tschermaks Mineralogische und Petrographische Mitteilungen*, **26**, 11–19.

Walenta, K. and Wimmenauer, W. (1961) Der Mineralbestand des Michaelganges im Weiler bei Lahr (Schwarzwald). [Translation: The mineral occurrences of the Michael Mine at Weiler near Lahr (Black Forest)]. *Jahreshefte des Geologischen Landesamts in Baden-Wuerttemberg*, **4**, 7–37.

[*Manuscript received 5 February 2003: revised 16 July 2003*]